HHS Public Access

Author manuscript

*Mar Pollut Bull*. Author manuscript; available in PMC 2016 November 15.

Published in final edited form as:

*Mar Pollut Bull*. 2015 November 15; 100(1): 445–452. doi:10.1016/j.marpolbul.2015.08.007.

# Spatial and vertical distribution of metals in sediment cores from Río Espíritu Santo estuary, Puerto Rico, United States

**Nekesha Williams** and **Karin A. Block***

Department of Earth and Atmospheric Sciences, The City College of New York, New York, NY 10031

## Abstract

The concentration and distribution of Cd, Cr, Cu, Fe, Mn, Ni, Pb, and Zn were investigated in three sediment cores representing 100–150 years of accumulation in upriver, midriver, and estuarine environments in Río Espíritu Santo (RES), Puerto Rico. Grain-size distribution, organic matter and carbonate content were determined to assess their influence on metal concentrations. Minimum biotoxicity levels of Ni and Cu were exceeded in the upriver and midriver sites, while the minimum biotoxicity level of Cu was exceeded in the estuarine location. Pb concentration decreased by ~35 % in the upper portion of the midriver and estuarine cores compared to downcore concentrations as a consequence of leaded gasoline regulation. Enrichment Factors and Geoaccumulation Indices were calculated for each metal revealing high levels of Cu in all three cores, likely from an igneous source. Our results provide a baseline for metal contamination in an area facing further land use change.

### Keywords

Puerto Rico; Metals; Estuary; Sediment; Pollution; Caribbean

Sediments transporting contaminants from terrestrial areas can enter coastal and marine systems, compromising ecosystem health and function (Birch and Olmos, 2008; Chapman and Wang, 2001). The Commonwealth of Puerto Rico is a territory of the United States comprised of several islands, including mainland Puerto Rico, Culebra, Vieques, and Mona. The mainland (hereafter, Puerto Rico) is characterized by a large population density along the coast and a strong dependence on coastal resources for food and tourism; therefore, water and sediment quality in the terrestrial and marine domains are of particular importance (Gould et al., 2012).

Puerto Rico is tropical and subject to high rainfall during its rainy season from April through November. Easterly trade winds and a mountain range that stretches east to west across the island produces a rain shadow along the southern coast and highest rainfall amounts in the

*corresponding author: kblock@ccny.cuny.edu; ph: 212-650-8543; fax: 212-650-6482.

northeast region. The more arid south shore of the island is subject to significant rainfall during hurricane season (June to November) as a result of tropical depressions.

Puerto Rico has undergone dramatic changes in land use over the last 100 years. Rapid population growth and deforestation to increase arable land (Grau et al., 2003) for the production of sugarcane, plantain, and coffee (Grau et al., 1997) have resulted in a decline in the forested area to only 6% of the landscape by the 1940s (France et al., 1997; Helmer, 2004). A shift to an industrial economy after 1945 led to some reforestation; however, population growth in urban and suburban areas has given rise to other environmental issues such as pollution (Hunter and Arbona, 1995; Uriarte et al., 2011). Currently, Puerto Rico is experiencing an economic depression that has seen the decline of its industrial economy and a greater focus on tourism. Northeastern Puerto Rico, in particular, is of primary importance to the tourism industry. Since 2002, the commonwealth has invested over $2.2 billion in new resorts and golf courses, mostly concentrated in the “golf corridor” in the northeastern coast of Puerto Rico. Three of these new resorts, the St. Regis Bahia Beach, the Gran Melia Golf Resort, and the Trump International Golf Club built in 2010, 2004, and 2006, respectively, sit at the mouth of the Rio Espiritu Santo and are adjacent to the government-designated Rio Espiritu Santo (RES) Natural Reserve. Further development plans include adding a private inland marina within the estuary and two artificial beaches that would remove seagrass from the site (Hernández-Delgado et al., 2012).

The RES Natural Reserve was established in 1985 by resolution of the Puerto Rico Planning Board and comprises a total surface area of 9,668 hectares that includes emergent and submerged lands, most of which are owned by a total of 39 landowners (Aguilar-Perera et al., 2006; Ventosa-Febles et al., 2005). Marine Protected Areas in Puerto Rico can include natural reserves, insular forests, critical habitats, no-take zones (Aguilar-Perera et al., 2006). The reserve provides important fisheries and nursing habitat for amphidromous, nearshore, and marine species. Sixty-seven bird species, two reptile species, two amphibian species, 24 invertebrates including crustaceans, and 81 fish species have been reported (Ventosa-Febles et al., 2005). Goenaga et al. (1989), and Hernandez-Delgado (2001) have documented the deterioration of the coral reef communities of the RES estuary.

Given the ongoing economic stress on the island and the increasing interest in tourism further development of the land surrounding the RES may pose a significant risk to this vulnerable ecosystem. This study examines metal concentrations in sediment cores from three sites along the RES, one of the nine rivers draining the Caribbean National Forest (CNF) in Rio Grande. Rio Grande is a municipality on the northeast coast of Puerto Rico with one of the highest population densities in Puerto Rico (345.88 persons/$km^2$; U.S. Census Bureau, 2013).

We provide the first assessment of trace heavy metal chemistry of three sediment cores that capture 100–150 years of sediment accumulation along a longitudinal profile of the RES that represents a hydraulic gradient (freshwater-brackish-marine). Our goal is to document the temporal variability in metal accumulation in this linear fluvial-estuarine-coastal system. Our data provides a historical context for the flux and depositional history of sediments and heavy metals, which will serve as baseline for evaluating potential impacts of future

development in the area. Our data can also provide a reference for comparing metals accumulation to other areas in Puerto Rico and similar freshwater-brackish-marine systems in the region.

Three sediment cores were manually collected in June and July of 2007 and in August 2008 using a polycarbonate push-corer by wading to the sampling locations. Coring sites were selected based on accessibility to the stream channel, with the goal of capturing the range of hydraulic variability across freshwater, intermediate, and estuarine environments. Sediment cores were collected using individual polycarbonate push-corers. Core lengths varied due to inherent differences in substratum. Cores were extruded at local field stations after collection. The upper 10 cm of each core was sliced into 0.5 cm and 1 cm sections using a PVC spatula. No evidence of bioturbation or infauna was found in any of the cores. Core subsamples (sections) were immediately placed in pre-labeled plastic bags, and stored in iceboxes until shipped to laboratory where they were frozen at −20 °C. Thereafter, samples were freeze-dried and stored for further analysis.

Subsamples were analyzed for grain size, organic matter, and calcium carbonate content. Grain-size distribution was determined by wet-sieving samples through a 63 μm mesh sieve. Particles larger than 63 μm were categorized as sand and gravel. Percent silt and clay was determined on fine-grained material (< 63 μm) using a particle size analyzer (Micromeritics, Saturn DigiSizer 5200, Norcross, Georgia). Sequential weight loss on ignition (LOI) was used to determine organic matter at 550 °C and calcium carbonate content at 950 °C; (Dean Jr, 1974; Heiri et al., 2001).

Samples were prepared for chemical analysis by reflux following US EPA Method 200.8 (USEPA, 1999). Cd, Cr, Cu, Mn, Ni, Pb, and Zn concentrations were determined by inductively coupled plasma-mass spectrometer (ICP-MS) on a Thermo Fisher Scientific X-Series 2 instrument. Quality control was achieved by monitoring of a five-point calibration curve and a multi-element standard (SPEX CertiPrep, Inc. Metuchen, New Jersey). Reagent blanks were interspersed with sediment samples during instrument runs. Iron concentrations were determined by atomic absorption on a ThermoScientific Atomic Absorption Spectrometer in flame mode. For all metals, the reported concentrations represent an average of three determinations. The average relative standard deviations and detection limits for each metal are reported in Supplementary Table A2.

Descriptive statistics were generated for grain-size distribution, organic matter, carbonate content, and metal concentrations. Square root transformation was applied for all elements in preparation of parametric tests. A one-way ANOVA was conducted on each metal to test for differences in metal concentrations across the three cores. Pearson correlation analysis was conducted between all pairwise combinations of metals, silt, clay, and organic matter. Statistical significance from all analyses was determined at $p < 0.05$

The degree of metal contamination in sediment samples was assessed using the Geoaccumulation Index ($I_{geo}$; Müller, 1969; Equation 1) and the Enrichment Factor (EF). $I_{geo}$ was computed as:

$$I_{geo}=Log_2\left([C_n]/1.5(B_n)\right) \quad \text{Equation (1)}$$

where $C_n$ is the measured concentration of the trace element in sediments, $B_n$ is the average background value of element $n$ in shale (Turekian and Wedepohl, 1961), 1.5 is a correction factor applied to address lithogenic effects (Lin et al., 2008). The (Förstner et al., 1993) classification for geoaccumulation is utilized here to evaluate $I_{geo}$ from RES.

EF is widely used to determine sediment contamination by metals (Çevik et al., 2009; Chatterjee et al., 2007; Garcia et al., 2009; Magesh et al., 2011; Rubio et al., 2000), in spite of the limitations presented by Reimann and De Caritat (2005). EF has been also been used in volcanic islands like Puerto Rico to determine anthropogenic versus geogenic enrichment of trace elements in two species of lichens in Italy (Varrica et al., 2000), and to determine atmospheric and pedogenic influence on concentration of heavy metals in soils of a remote oceanic island, Fernando do Norohna, Brazil (Oliveira et al., 2011). Contamination is determined by comparing measured concentration to background values in crustal or shale matrices. The EF for a given metal is computed as:

$$EF=([Me_s]/[Fe_s])/([Me_{shale}/Fe_{shale}]) \quad \text{Equation (2)}$$

where $Me_s$ and $Fe_s$ represent the concentrations of total metal (Me) and iron (Fe) in sediment samples. $Me_{shale}$ and $Fe_{shale}$ represent the background metal and Fe concentrations in shale. In this study, Fe was used to normalize metal concentrations because of its abundance in soils for this area (Chacon et al., 2006). The Sutherland (2000) classification was used to evaluate the degree of contamination associated with the computed enrichment factors.

Sediment cores contained admixtures of sand and gravel, silt, and clay-size particles (Table 1). Average clay content was highest (~22%) in Core 1 at the upriver sampling site; mid-river Core 2 contained the highest average silt content (~ 61%) and 19% clay content; Core 3 (estuarine location) contained the highest average total sand and gravel content (~ 36%). The spatial variation in grain-size distribution reflects changes in the hydraulic environment. The dominance of fine-fraction (clay plus silt) in Cores 1 and 2 suggests that lower-energy settings are prevalent in the upper portion of the system, whereas higher sand-gravel content in Core 3 reflects the higher-energy environment within the lower fluvial-estuarine system.

Organic Matter (OM) ranged from approximately 10 to 16 wt. % in Core 1, 12 to 20 wt. % in Core 2, and 13 to 25% in Core 3. Carbonate content ranged from 1.7 to 2.8 wt. % in Core 1, with the exception of a sample at 10 cm depth that contained 6 wt. %. Core 2 carbonate ranged from 2.25 to 5 wt. % and Core 3 ranged from 2.7 to 6.5 wt. % (Table 1). The complete dataset for OM and carbonate content for each core is available in Table A1 in the Supplementary Materials. Vertical profiles of organic matter and carbonate content within each of the three cores are showed that both Cores 2 and 3 contained larger amounts of OM in surface samples and lower amounts at depth than Core 3 (Fig. 2). Overall, the carbonate content profiles for each core fell within a narrow 2–4 % range of mean carbonate. Core 3 possessed the highest carbonate content on average. The accumulation of OM in surface sediments of cores 2 and 3 is primarily due increase deposit of leaf litter from adjacent

mangroves. Core 3 was influence the most by tidal action and thus showed higher input and accumulation of carbonates (i.e., coral fragments).

The mean and standard deviation of trace metal concentrations within each of the sediment cores were generally lower than the average shale concentrations reported in Turekian and Wedepohl (1961) and lower than the effects-range low (ERL) and effects-range median (ERM) parameters (Long et al., 1995) for aquatic toxicity (Table 2). ERL concentrations are those below which little or no toxicity effects are generally observed and ERM are the concentrations above which adverse biological effects can be detected. The complete dataset is available in Table A2 in the Supplementary Materials. The mean concentrations showed low or no enrichment for Cd, Cr, Ni, Mn, Pb and Zn in all three cores, while mean Cu concentrations exceeded the average shale values in all three cores and Fe concentrations showed enrichment in Cores 1 and 2. Two elements exhibited potential biological toxicity effects: in all three cores, the average concentration of Cu was above the ERL and, in Core 3 concentrations at some depths approached or exceeded the ERM. Ni concentration exceeded ERL values in Cores 1 and 2, with the highest average concentration in Core 1, reflecting provenance from the igneous source.

An increase in mean Cd concentration and decrease in Fe concentrations in the seaward direction were also observed. The highest average Cd concentration was reported for core 3 (0.23 mg/kg). The relatively higher accumulation of Cd in Core 3 may be attributed to erosion of surface samples from upstream areas. Mean concentrations of Cu (156 mg/kg), Zn (83 mg/kg) and Mn (492 mg/kg) were also the highest in Core 3, but lowest in Core 2. Conversely, mean Fe concentrations decreased in the seaward direction with Core 1 containing the highest concentration (~7 %) on average. For the metals that did not show the seaward gradient, Core 1 had the highest mean concentrations of Cr (55mg/kg) and Ni (26 mg/kg) and Pb was similarly highest in cores 2 and 3 (13 mg/kg).

The concentration of all metals (except Pb) in all three cores fluctuated with depth, without showing obvious overall increasing or decreasing trends (Fig. 3). In Cores 1 and 2, concentrations of Cd, Cr, Mn, Ni, Pb, and Fe tracked or mirrored each other downcore. Similarities in distribution patterns among these elements may indicative of their chemical properties (transition metals). In Core 2, Mn concentration exhibited high variability and reached nearly double its average concentration at 33 cm depth; at 31 cm depth in Core 2, the Mn concentration was 3241 mg/kg, which we consider an analytical error. Additionally, Zn exhibited higher variability in Core 2 but was on average lower than in Cores 1 and 3. The average concentration of Pb in the lower part of Core 2 below 21 cm depth was 15.6 mg/kg, notably higher than in the upper part of the core where the average concentration was 9.5 mg/kg.

Three of the metals in Core 3 either showed very high variability (Cu) or evidence suggestive of external events (Mn and Pb). Cu concentration was highest and experienced the most fluctuation in Core 3, with peaks in concentration at 15 to 21 cm, 23 to 25 cm, and 37 to 39 cm depth. Mn concentration in Core 3 was relatively constant, with the exception of a large jump from 400 to 600 mg/kg between 25 cm and 45 cm depth, possibly due to a sudden increase in sediment input from a storm event. Pb concentration in Core 3 was

significantly higher below 27 cm depth (mean of 16.3 mg/kg versus 10.5 mg/kg in the upper part of the core corresponding a 35% decrease between lower and upper portions of the core and similar to the pattern observed in Core 2. Similar decreases in Pb in sediment cores in general are hypothesized to reflect regulation of leaded gasoline post-1970s (Callender and Metre, 1997; Callender and Rice, 2000).

One-way ANOVAs indicated that all metal concentrations, with the exception of Pb, were significantly different among the cores ($p < 0.01$). This suggests that the differences in hydrology and sedimentology among sampling sites influenced the accumulation of the metals.

Pearson correlation analyses identified varying degrees of relationship among metals and sediment characteristics. Similarities were identified across cores, but there were also notable differences. Strong positive associations between Mn and Pb and Mn and Fe were found in all three cores. The strong correlation for Fe and Mn is interpreted as a consequence of the natural affinity of the two metals for oxyhydroxide formation. Additionally, both Mn and Fe were strongly associated with clay-size particles in the sediment matrix in all three cores, which confirms that Mn-Fe hydroxides are adsorbed to the surfaces of particles. Cu was positively correlated with silt-size particles in all three cores.

Cd showed significant, positive correlations with most metals (Cr, Fe, Mn, Ni, and Pb) in Core 1, the exceptions being Cu and Zn, which were negative and statistically significant (Table 3). Cu was also negatively correlated with both Fe and Pb, but not with Mn. This result suggests that Cu may be primarily adsorbed to in the Mn-hydroxides in the sediment matrix. Grain-size and OM content influenced trace metal distribution in Core 1, with all metals, except Ni and Fe, positively correlated to silt content. Cd, Cr, Cu, Pb, and Zn were positively correlated to OM content. All metals, except Pb and Zn, were positively correlated to clay-sized particles. Cd, Cr, Cu, Pb were positively correlated with OM, while Zn. Fe, Ni, and Mn were negatively correlated with OM.

Similar to Core 1, Cd was positively correlated to Cr, Ni, Zn, Cu, Fe, Mn, and Pb (Table 4). Unlike Core 1, Cu was positively (not negatively) associated with Fe and there was no association between Cu and clay in Core 2. Cd, Cu, Fe, Mn, and Pb were, like Core 1, positively correlated to silt and clay fractions, while Cr, Ni and Zn were negatively correlated. Negative correlations were found between Ni and clay, Ni and silt, Zn and clay, and between OM and all metals.

The correlations in Core 3 differed from those found in Cores 1 and 2 (Table 5). While negative correlations were reported between Cd and Cu and Cd and Zn (Core 1), as well as between Cd and Ni (Core 2), Core 3 showed negative correlations between Cd and all three metals. This suggests that the transport behavior of these metals differed between Cores 3 and Cores 1 and 2. Ni and Zn were negatively correlated with all sediment characteristics (clay, silt and OM) and Cu was primarily associated with silt-sized particles. No relationship was found between Fe and Cu and between Fe and Ni in Core 3, which differs from both Cores 1 and 2 and suggests that Fe-hydroxides did not influence the distribution of the Cu

and Ni at Core 3. Similar to Core 2, Ni and Zn were negatively correlated with all sediment characteristics (clay, silt and OM). All other metals (Cd, Cr, Fe, Mn and Pb) were positively correlated with grain-size (clay and silt) and OM content.

Average $I_{geo}$ values for each core indicated that all metals (Cd, Cr, Fe, Mn, Ni, Pb, Zn) with the exception of Cu occurred below contamination levels (Table 6). $I_{geo}$ values calculated for Cu in the sediment cores ranged from 0.59 to 1.05. The $I_{geo}$ values for Fe in all three cores were close to zero, which suggests that Fe behaved conservatively in the estuarine environment and supports using Fe for normalization in EF analysis.

EF values showed that all analyzed metals, with the exception of Cu, were either deficient or minimally enriched. Possible anthropogenic sources of Cu near the sampling sites include release from anti-fouling boat paint and influx from fungicide use in farming in the watershed. However, a anthropogenic source for the Cu, while possible, is unlikely. Cu was moderately enriched in all three hydrologic environments, and there are no major marinas in the estuary or nearby bay (Ensenada Comezón), and no significant agricultural activity in the watershed. The incidence of high Cu EF values in all three cores, in the absence of high values for other chemical indicators of anthropogenic contamination, point toward a geologic or bedrock source for this metal. Mineable copper porphyry deposits are found in several locations across the central mountain ranges of Puerto Rico, with a copper/gold porphyry and copper skarn within a few kilometers of the RES Watershed (Marsh, 1998). Based on this evidence, we propose that a Cu deposit on the northern flank of the Luquillo Mountains may be the source of anomalous Cu concentrations found in this study, and possibly presenting a natural toxicity threat to coastal biota near the RES estuary.

Spatiotemporal analysis of metals in the RES revealed that, on average, the fluvial-estuarine system contains low levels of contamination. A low energy hydrologic environment, as reflected in grain size distributions, dominated the upper and midriver locations, while the estuarine core was subject to a higher energy hydrologic environment resulting in a larger fraction of sand and gravel. The prevalence of fine grained sediments in the upper and midriver regimes appear to have influenced the longitudinal distribution of metals, promoting aggregation and settling of Cd, Cr, Mn, Ni, Pb, and Fe in Cores 1 and 2.

Core 2 located midriver contained the highest fraction of fine-grained sediments. However, clay and silt in this core did not correlate with metal content or OM. This suggests a rapid drop in water velocity, which leads to abrupt settling of fines and impacting the ability for OM and metals to aggregate with sediment.

Intermetallic relationships were distinct within each of the three cores. Combined with the strong positive and negative correlations among metals and the overall low levels of contamination in RES, this suggests that the downstream transport regime, as dictated by topography and the resulting grain size distribution, was a strong driver of metal concentrations in the sediments. While the fine fraction (silt and clay) correlated with a large number of metals in Cores 1 and 3, the correlation is absent in Core 2 despite having the highest relative amount of fine-grained sediments. A notable relationship is the strong correlation of Fe with Mn for Cores 1 and 2, but absent in Core 3. This suggests that the

hydrologic and geochemical conditions favored the aggregation and deposition of these two metals in tandem in the upriver and midriver settings, but not in the downriver (estuarine) environment. Mn–Fe variation and distinct fields roughly correspond typical trends in each environment are shown in Fig. 4. Upriver (primarily Core 1 sediments) sediments occupy a high Fe, high Mn cluster (horizontal line pattern). Midriver sediments occur in all three fields; however, a large number are characterized by low Mn concentrations (cross pattern). Some sediment from Cores 1 and 2, and the majority of sediments from Core 3, form a downriver/seaward array (diagonal line pattern) characterized by low Fe and high Mn concentrations.

A downriver increase in carbonate content may lead to precipitation of $MnCO_3$ in the sediment without co-precipitation with Fe. Downriver decreases in Fe, Ni, and Cr, all of which are likely to have weathered from the source igneous rocks, may be the result of fast settling in the upper regime of the stream, leading to depletion as the stream moves away from the source.

Despite generally low metals contamination levels in RES, average Cu concentration exceeded the level found at the contaminated site in San José Lagoon, PR (Acevedo-Figueroa et al., 2006). Because Cu concentration does not correlate with any other metal contaminants nor are there potential sources of Cu such as fungicide in the watershed or boating activity in the estuary, we hypothesize that the Cu contamination is of natural origin. In the estuarine core, spikes in Cu concentration reach ERM levels, which may be driven by higher salinity in this environment (Du Laing et al., 2009). The naturally high Cu concentrations in all the cores can be explained by the existence of copper deposits in the northern Luquillo Mountains within a few kilometers of the RES watershed (Marsh, 1998).

Radioisotopic dating of Core 3 only using $^{210}Pb$ showed that it represented about 100 to 150 years of sedimentation and heavy metal accumulation. We used the constant rate of supply model (CRS model) constrained by $^{210}Pb$ (See Supplemental Table A3). Given the lower rates of sediment accumulation in the farther upstream cores, Cores 2 and 3 also reflect at least 100 to 150 years of sediment accumulation. This time period captures variation in heavy metal accumulation during pre-industrial times in Puerto Rico (before 1940s) to the recent past (2007), and provides a coarse time scale for interpreting the three cores.

Table 7 shows the average concentrations of metals in sediments reported for other studies in Puerto Rico and Jamaica. The concentrations of all metals in RES are higher than in uncontaminated sites in Jobos Bay, PR, (Aldarondo-Torres et al., 2010; Apeti et al., 2012) and Joyuda, PR (Acevedo-Figueroa et al., 2006), except for Mn which is higher in Jobos Bay (Apeti et al., 2012). In the uncontaminated site of La Parguera, PR (Pait et al., 2008), Ni exceeded average concentrations found in RES. In Montego Bay, Jamaica, (Jaffé et al., 2003) also found that Cd and Ni occurred at higher levels than in RES. In Guánica Bay, PR, levels of Cr and Ni are considerably higher than in RES (Whitall et al., 2014), while Mn levels are comparable. In fact, Cr and Ni in Guánica Bay, PR, which are some of the highest measured in the U.S., are attributed to the source bedrock (Whitall et al., 2014). Our results provide a baseline dataset for metals accumulation predating the industrialization of PR to the near-present for key locations in the RES, which can be used to compare to other

locations and to assess the effects of future activities in the Caribbean National Forest area on metals contamination.

## Supplementary Material

Refer to Web version on PubMed Central for supplementary material.

## Acknowledgments

This work was supported in part by an NSF-AGEP Postdoctoral Fellowship to Nekesha Williams; and NIH Research Centers in Minority Institutions (NIH/NCRR/RCMI) CCNY/Grant G12-RR03060. Our sincere thanks to Dr. Al Katz and Dr. Kenneth A. Rose for their critical review and helpful comments.

## References

United States Census Bureau, New York; Department of Labor. Population of Puerto Rico. 2013. Retrieved October 10, 2014http://www.census.gov/popest/

Acevedo-Figueroa D, Jiménez BD, Rodríguez-Sierra CJ. Trace metals in sediments of two estuarine lagoons from Puerto Rico. Environmental Pollution. 2006; 141:336–342. [PubMed: 16249046]

Aguilar-Perera A, Schärer M, Valdés-Pizzini M. Marine protected areas in Puerto Rico: Historical and current perspectives. Ocean & Coastal Management. 2006; 49:961–975.

Aldarondo-Torres JX, Samara F, Mansilla-Rivera I, Aga DS, Rodríguez-Sierra CJ. Trace metals, PAHs, and PCBs in sediments from the Jobos Bay area in Puerto Rico. Marine Pollution Bulletin. 2010; 60:1350–1358. [PubMed: 20638083]

Apeti D, Whitall D, Pait A, Dieppa A, Zitello A, Lauenstein G. Characterization of land-based sources of pollution in Jobos Bay, Puerto Rico: status of heavy metal concentration in bed sediment. Environ Monit Assess. 2012; 184:811–830. [PubMed: 21509514]

Birch GF, Olmos MA. Sediment-bound heavy metals as indicators of human influence and biological risk in coastal water bodies. ICES Journal of Marine Science: Journal du Conseil. 2008; 65:1407–1413.

Callender E, Metre PCV. Environmental policy analysis, peer reviewed: reservoir sediment cores show US lead declines. Environmental science & technology. 1997; 31:424A–428A.

Callender E, Rice KC. The urban environmental gradient: anthropogenic influences on the spatial and temporal distributions of lead and zinc in sediments. Environmental Science & Technology. 2000; 34:232–238.

Çevik F, Göksu M, Derici O, Fındık Ö. An assessment of metal pollution in surface sediments of Seyhan dam by using enrichment factor, geoaccumulation index and statistical analyses. Environ Monit Assess. 2009; 152:309–317. [PubMed: 18478346]

Chacon N, Silver W, Dubinsky E, Cusack D. Iron Reduction and Soil Phosphorus Solubilization in Humid Tropical Forests Soils: The Roles of Labile Carbon Pools and an Electron Shuttle Compound. Biogeochemistry. 2006; 78:67–84.

Chapman PM, Wang F. Assessing sediment contamination in estuaries. Environmental Toxicology and Chemistry. 2001; 20:3–22. [PubMed: 11351413]

Chatterjee M, Silva Filho EV, Sarkar SK, Sella SM, Bhattacharya A, Satpathy KK, Prasad MVR, Chakraborty S, Bhattacharya BD. Distribution and possible source of trace elements in the sediment cores of a tropical macrotidal estuary and their ecotoxicological significance. Environment International. 2007; 33:346–356. [PubMed: 17196656]

Dean WE Jr. Determination of carbonate and organic matter in calcareous sediments and sedimentary rocks by loss on ignition: comparison with other methods. Journal of Sedimentary Research. 1974; 44

Du Laing G, Rinklebe J, Vandecasteele B, Meers E, Tack FMG. Trace metal behaviour in estuarine and riverine floodplain soils and sediments: A review. Science of The Total Environment. 2009; 407:3972–3985. [PubMed: 18786698]

Förstner U, Ahlf W, Calmano W. Sediment quality objectives and criteria development in Germany. Water Science and Technology. 1993; 28:307–316.

France, DR.; Weaver, PL.; Eggen-McIntosh, S. Resource Bulletin. Asheville, NC: 1997. Forest Resources of Puerto Rico, 1990, US Department of Agriculture, Forest Service, Southern Research Station.

Garcia CAB, Barreto MS, Passos EA, Alves JdPH. Regional geochemical baselines and controlling factors for trace metals in sediments from the Poxim River, Northeast Brazil. Journal of the Brazilian Chemical Society. 2009; 20:1334–1342.

Goenaga C, Vicente VP, Armstrong RA. Bleaching induced mortalities in reef corals from La Parguera, Puerto Rico: A precursor of change in the community structure of coral reefs? Caribbean Journal of Science. 1989; 25:59–65.

Gould, WA.; Martinuzzi, S.; Parés-Ramos, IK. Land Use, Population Dynamics, and Land-Cover Change in Eastern Puerto Rico. In: Murphy, SF.; Stallard, RF., editors. Water Quality and Landscape Processes of Four Watersheds in Eastern Puerto Rico. USGS Professional Paper. 2012. p. 25-42.

Grau HR, Aide TM, Zimmerman JK, Thomlinson JR, Helmer EH, Zou X. The ecological consequences of socioeconomic and Land-use changes in postagriculture Puerto Rico. BioScience. 2003; 53:1159–1168.

Grau HR, Arturi MF, Brown AD, Aceñolaza PG. Floristic and structural patterns along a chronosequence of secondary forest succession in Argentinean subtropical montane forests. Forest ecology and management. 1997; 95:161–171.

Heiri O, Lotter A, Lemcke G. Loss on ignition as a method for estimating organic and carbonate content in sediments: reproducibility and comparability of results. Journal of Paleolimnology. 2001; 25:101–110.

Helmer EH. Forest conservation and land development in Puerto Rico. Landscape Ecol. 2004; 19:29–40.

Hernandez-Delgado, E. Areas Marinas Protegidas en Puerto Rico: El oscuro abismo entre el papel y el mundo real. XXIV Simposio Recursos Naturales; 2001. p. 98-123.

Hernández-Delgado, EA.; Ramos-Scharrón, CE.; Guerrero-Pérez, CR.; Meléndez-Díaz, JO.; Lucking, MA.; Méndez-Lázaro, PA.; Laureano, R. Long-Term Impacts of Non-Sustainable Tourism and Urban Development in Small Tropical Islands Coastal Habitats in a Changing Climate: Lessons Learned from Puerto Rico. INTECH Open Access Publisher; 2012.

Hunter JM, Arbona SI. Paradise lost: an introduction to the geography of water pollution in Puerto Rico. Social Science & Medicine. 1995; 40:1331–1355. [PubMed: 7638643]

Jaffé R, Gardinali PR, Cai Y, Sudburry A, Fernandez A, Hay BJ. Organic compounds and trace metals of anthropogenic origin in sediments from Montego Bay, Jamaica: assessment of sources and distribution pathways. Environmental Pollution. 2003; 123:291–299. [PubMed: 12628208]

Lin C, He M, Zhou Y, Guo W, Yang Z. Distribution and contamination assessment of heavy metals in sediment of the Second Songhua River, China. Environ Monit Assess. 2008; 137:329–342. [PubMed: 17508261]

Long E, Macdonald D, Smith S, Calder F. Incidence of adverse biological effects within ranges of chemical concentrations in marine and estuarine sediments. Environmental Management. 1995; 19:81–97.

Magesh NS, Chandrasekar N, Vetha Roy D. Spatial analysis of trace element contamination in sediments of Tamiraparani estuary, southeast coast of India. Estuarine, Coastal and Shelf Science. 2011; 92:618–628.

Marsh, SP. Stream-Sediment Geochemistry of Puerto Rico, Isla De Vieques, And Isla De Culebra. In: Bawiec, WJ., editor. Geology, Geochemistry, Geophysics, Mineral Occurrences and Mineral Resource Assessment for the Commonwealth of Puerto Rico. USGS; 1998. p. 337

Müller G. Index of geo-accumulation in sediments of the Rhine River. Geojournal. 1969; 2:108–118.

Oliveira S, Pessenda LCR, Gouveia SEM, Favaro DIT. Heavy metal concentrations in soils from a remote oceanic island, Fernando de Noronha, Brazil. Anais da Academia Brasileira de Ciências. 2011; 83:1193–1206.

Pait AS, Whitall DR, Jeffrey CFG, Caldow C, Mason AL, Lauenstein GG, Christensen JD. Chemical contamination in southwest Puerto Rico: An assessment of trace and major elements in nearshore sediments. Marine Pollution Bulletin. 2008; 56:1953–1956. [PubMed: 18845309]

Reimann C, de Caritat P. Distinguishing between natural and anthropogenic sources for elements in the environment: regional geochemical surveys versus enrichment factors. Science of The Total Environment. 2005; 337:91–107. [PubMed: 15626382]

Rubio B, Nombela MA, Vilas F. Geochemistry of Major and Trace Elements in Sediments of the Ria de Vigo (NW Spain): an Assessment of Metal Pollution. Marine Pollution Bulletin. 2000; 40:968–980.

Sutherland RA. Bed sediment-associated trace metals in an urban stream, Oahu, Hawaii. Environmental Geology. 2000; 39:611–627.

Turekian KK, Wedepohl KH. Distribution of the Elements in Some Major Units of the Earth's Crust. Geological Society of America Bulletin. 1961; 72:175–192.

Uriarte M, Yackulic CB, Lim Y, Arce-Nazario JA. Influence of land use on water quality in a tropical landscape: a multi-scale analysis. Landscape Ecol. 2011; 26:1151–1164.

Varrica D, Aiuppa A, Dongarra G. Volcanic and anthropogenic contribution to heavy metal content in lichens from Mt. Etna and Vulcano island (Sicily). Environmental Pollution. 2000; 108:153–162. [PubMed: 15092945]

Ventosa-Febles, EA.; Camacho Rodriguez, M.; Chabert Llompart, JL.; Sustache Sustache, J.; Davial Casanova, D. Puerto Rico Critical Wildlife Areas. Commonwealth of Puerto Rico Department of Natural and Environmental Resources Bureau of Fish and WildlifeTerrestrial Resources Division; San Juan, Puerto Rico: 2005.

Whitall D, Mason A, Pait A, Brune L, Fulton M, Wirth E, Vandiver L. Organic and metal contamination in marine surface sediments of Guanica Bay, Puerto Rico. Mar Pollut Bull. 2014; 80:293–301. [PubMed: 24447634]

## Highlights

- A suite of trace metals was analyzed in upriver, midriver and estuarine cores.
- Minimum biotoxicity levels of Ni were exceeded in the upriver and midriver sites.
- Biotoxicity levels of Cu exceeding ERL were found in all three sites.
- Pb decreased ~ 35% in the upper portion of the midriver and estuary cores.
- High levels of Cu contamination are likely of natural origin.

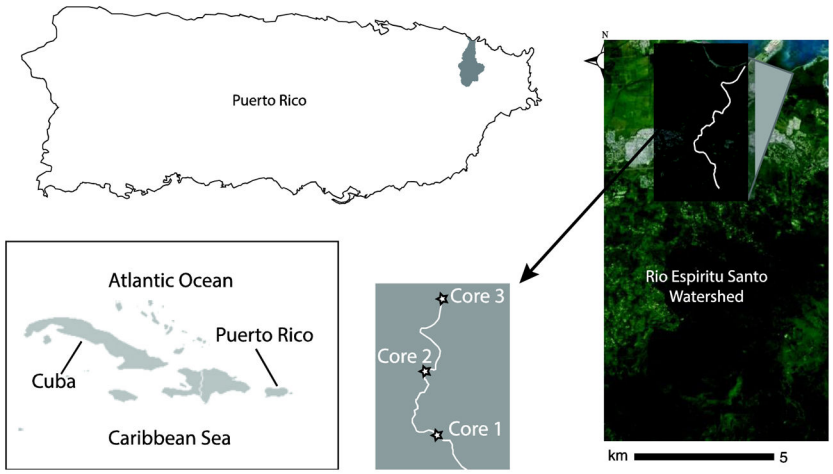


**Figure 1.**

Map of study area with inset showing location of the Río Espíritu Santo watershed and sampling locations. Modified map of Greater Antilles used by permission: Creative Commons License SA-3.0.

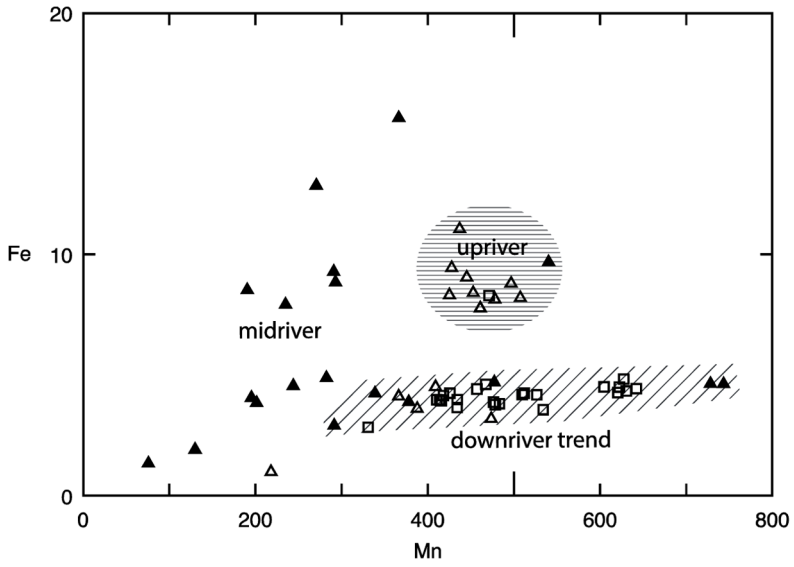


**Figure 2.**

Vertical profiles for organic matter and calcium carbonate content (wt. %) in all three sediment cores. Core 1 profile is represented by solid black lines, Core 2 by solid grey lines, and Core 3 by dashed black lines.

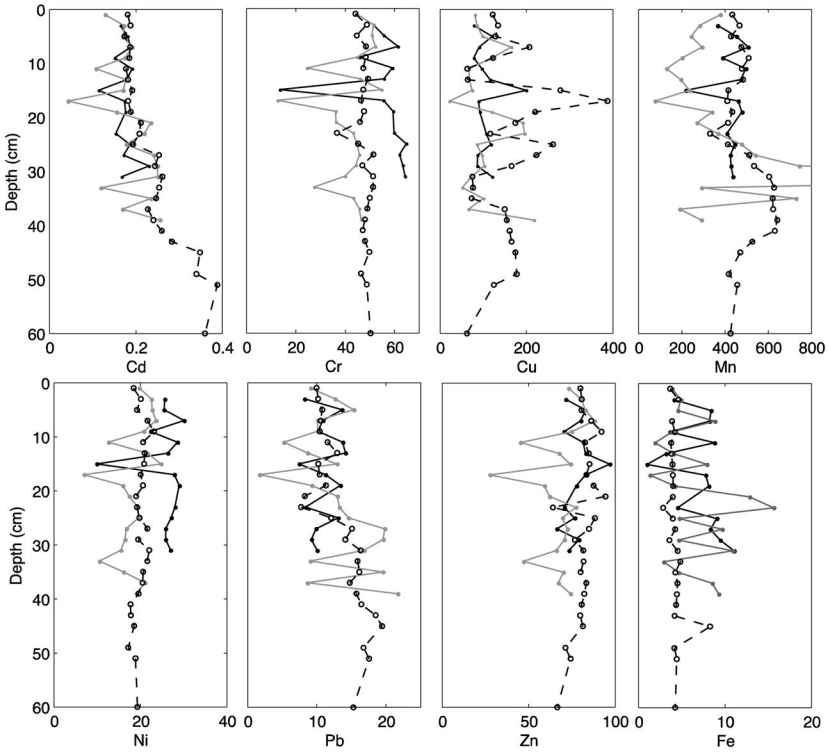


**Figure 3.**

Depth profiles of Cd, Cr, Cu, Mn, Ni, Pb, Zn (mg/kg) and Fe (wt. %) concentrations. Mn concentration in Core 2 at 31 cm (off-scale) is 3241 mg/kg. Symbols and grayscale colors are the same as in Fig. 2.

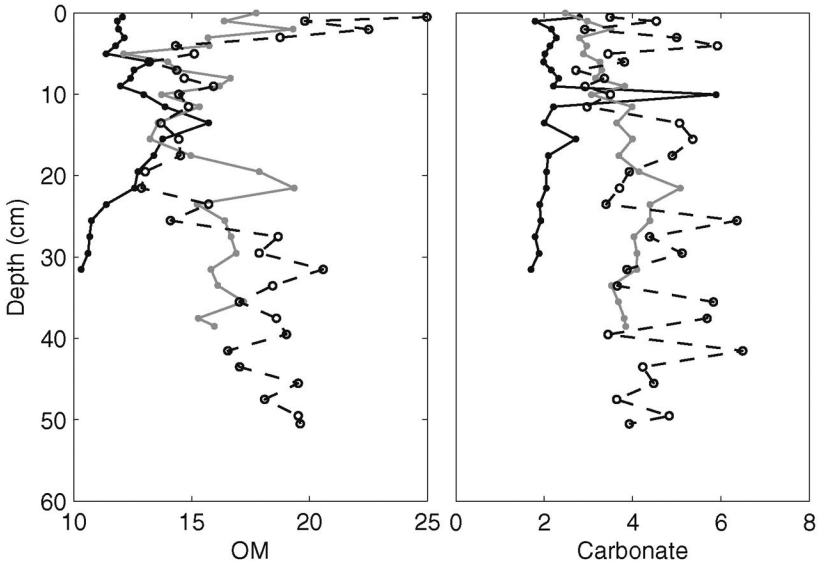


**Figure 4.**

Mn – Fe variation in core sediments. Concentrations are in mg/kg. Core 1 sediments are represented by open triangles, Core 2 sediments are represented by filled triangles, and Core 3 are represented by open squares. The horizontal line pattern primarily captures sediments characteristic of upriver environment, stippled pattern represents midriver sediments and diagonal pattern indicates a downriver trend primarily occupied by midriver and estuarine sediments.

**Table 1**

Average values for sand and gravel, silt, clay, organic matter and calcium carbonate content (%) in samples from three sediment cores

| Environment | Core | % Sand + Gravel | % Silt | % Clay | % Fine Fraction | % OM | % Carbonate |
|---|---|---|---|---|---|---|---|
| Up-River | Core 1 | 27 | 51 | 22 | 73 | 12 | 2 |
| Intermediate | Core 2 | 20 | 61 | 19 | 80 | 16 | 4 |
| Mouth - Estuary | Core 3 | 35 | 49 | 16 | 64 | 17 | 4 |

**Table 2**

Mean and standard deviation of trace metal concentrations in sediments. All concentrations are expressed in units of ppm with the exception of Fe (%)

| Sample | N | Cd | Cr | Cu | Ni | Pb | Zn | Mn | Fe |
|---|---|---|---|---|---|---|---|---|---|
| Core 1 | 14 | 0.13 ± 0.03 | 55 ± 13.0 | 106 ± 31.0 | 26 ± 4.90 | 11 ± 2.29 | 78 ± 7.67 | 428 ± 72.1 | 6.82 ± 2.94 |
| Core 2 | 20 | 0.18 ± 0.06 | 42 ± 11.4 | 104 ± 51.3 | 18 ± 4.47 | 13 ± 5.20 | 68 ± 14.1 | 474 ± 669 | 6.46 ± 3.80 |
| Core 3 | 26 | 0.23 ± 0.06 | 47 ± 3.57 | 156 ± 75.5 | 20 ± 1.45 | 13 ± 3.29 | 83 ± 6.78 | 492 ± 85.8 | 4.27 ± 0.93 |
| Average Shalea | | 0.3 | 90 | 45 | 68 | 20 | 95 | 850 | 4.72 |
| ERLb | | 1.2 | 81 | 34 | 20.9 | 46.7 | 150 | na | na |
| ERMb | | 9.6 | 370 | 270 | 51. 6 | 218 | 410 | na | na |

[a] Turekian and Wedepohl (1961)

[b] Long et al. (1995)

*Mar Pollut Bull*. Author manuscript; available in PMC 2016 November 15.

**Table 3**

Pearson correlation coefficient values between metals, silt, clay and organic matter for Core 1

| | Cd | Cr | Cu | Fe | Mn | Ni | Pb | Zn | Silt | Clay | OM |
|---|---|---|---|---|---|---|---|---|---|---|---|
| Cd | 1 | | | | | | | | | | |
| Cr | 0.79** | 1 | | | | | | | | | |
| Cu | −0.58* | −0.71 | 1 | | | | | | | | |
| Fe | 0.76** | 0.81** | −0.46 | 1 | | | | | | | |
| Mn | 0.77** | 0.89** | 0.62* | 0.75** | 1 | | | | | | |
| Ni | 0.73** | 0.92** | 0.74** | 0.74** | 0.94** | 1 | | | | | |
| Pb | 0.48** | 0.47 | −0.15* | 0.44 | 0.73** | 0.51 | 1 | | | | |
| Zn | −0.21** | 0.63* | 0.70** | 0.35 | 0.34 | −0.56* | 0.12 | 1 | | | |
| Silt | 0.20** | 0.47 | 0.4 | −0.48 | 0.16 | −0.39 | 0.36 | 0.66* | 1 | | |
| Clay | 0.36 | 0.53 | 0.12 | 0.55* | 0.25 | 0.31 | −0.03 | −0.53* | −0.45 | 1 | |
| OM | 0.25 | 0.4 | 0.22 | −0.56* | −0.04 | −0.21 | 0.3 | 0.60* | 0.73** | 0.75** | 1 |

* significance level of $p < 0.05$

** significance level of $p<0.01$

**Table 4**

Pearson correlation coefficient values between metals, silt, clay and organic matter for Core 2.

| | Cd | Cr | Cu | Fe | Mn | Ni | Pb | Zn | Silt | Clay | OM |
|---|---|---|---|---|---|---|---|---|---|---|---|
| Cd | 1 | | | | | | | | | | |
| Cr | 0.47 | 1 | | | | | | | | | |
| Cu | 0.65** | 0.22 | 1 | | | | | | | | |
| Fe | 0.68** | 0.36 | 0.77** | 1 | | | | | | | |
| Mn | 0.57** | 0.19 | 0.06 | 0.14 | 1 | | | | | | |
| Ni | 0.24 | 0.91** | 0.24 | 0.33 | −0.18 | 1 | | | | | |
| Pb | 0.85** | 0.49** | 0.38 | 0.44 | 0.69** | 0.15 | 1 | | | | |
| Zn | 0.50* | 0.94** | 0.41 | 0.45 | 0.2 | 0.86** | 0.47 | 1 | | | |
| Silt | 0.36 | −0.38 | 0.1 | 0.23 | 0.47 | −0.52* | 0.33 | −0.46 | 1 | | |
| Clay | 0.19 | −0.47 | 0.01 | 0.15 | 0.36 | −0.61** | 0.2 | −0.52* | 0.91** | 1 | |
| OM | −0.44 | −0.7 | −0.21 | −0.38 | −0.32 | −0.52* | −0.47 | −0.64** | 0.11 | 0.2 | 1 |

* significance level of $p < 0.05$

** significance level of $p<0.01$

**Table 5**

Pearson correlation coefficient values between metals, silt, clay and organic matter for Core 3.

| | Cd | Cr | Cu | Fe | Mn | Ni | Pb | Zn | Silt | Clay | OM |
|---|---|---|---|---|---|---|---|---|---|---|---|
| Cd | 1 | | | | | | | | | | |
| Cr | 0.34 | 1 | | | | | | | | | |
| Cu | −0.19 | −0.17 | 1 | | | | | | | | |
| Fe | 0.49* | 0.54** | 0 | 1 | | | | | | | |
| Mn | 0.17 | 0.39 | −0.32 | 0.29 | 1 | | | | | | |
| Ni | −0.44* | 0.61** | 0.13 | −0.09 | 0.24 | 1 | | | | | |
| Pb | 0.79** | 0.34 | −0.21 | 0.59** | 0.60** | 0.24 | 1 | | | | |
| Zn | −0.53** | 0.34 | 0.33 | 0.14 | 0.22 | 0.47* | −0.23 | 1 | | | |
| Silt | 0.46* | 0.3 | 0.44* | 0.39 | 0.31 | −0.25 | 0.48* | −0.25 | 1 | | |
| Clay | 0.72** | 0.3 | −0.24 | 0.51** | 0.42* | −0.35 | 0.69** | −0.28 | 0.82** | 1 | |
| OM | 0.54** | 0.28 | −0.33 | 0.36 | 0.35 | −0.21 | 0.51** | −0.46 | 0.66** | 0.58* | 1 |

* significance level of $p < 0.05$

** significance level of $p<0.01$

## Table 6

Average enrichment factor (EF) and geoaccumulation index (Igeo) of trace metals in the three cores.

| Sample ID | EF | Igeo |
|---|---|---|
| **Core 1** | | |
| Cd | 0.54 | −1.39 |
| Cr | 0.49 | −1.37 |
| Cu | **3.03** | **0.59** |
| Fe | N/A | −0.29 |
| Mn | 0.45 | −1.6 |
| Ni | 0.03 | −2.3 |
| Pb | 0.52 | −1.48 |
| Zn | 0.91 | −0.87 |
| **Core 2** | | |
| Cd | 0.53 | −1.39 |
| Cr | 0.42 | −1.76 |
| Cu | **1.94** | **0.45** |
| Fe | N/A | −0.38 |
| Mn | 0.42 | −1.97 |
| Ni | 0.24 | −2.55 |
| Pb | 0.55 | −1.43 |
| Zn | 0.66 | −1.12 |
| **Core 3** | | |
| Cd | 0.89 | −0.95 |
| Cr | 0.6 | −1.5 |
| Cu | **3.99** | **1.05** |
| Fe | N/A | −0.17 |
| Mn | 0.65 | −1.39 |
| Ni | 0.33 | −2.36 |
| Pb | 0.75 | −1.19 |
| Zn | 0.74 | −0.81 |

**Table 7**

Average metal concentrations found in sediments in Puerto Rico and Jamaica (μg/g)

| Reference | Location | Environment | Cd | Cu | Cr | Ni | Mn | Pb | Zn | Fe* |
|---|---|---|---|---|---|---|---|---|---|---|
| This study | Río Espíritu Santo, PR | Riverine/Estuarine | 0.18 | 122 | 48 | 5.2 | 464 | 37 | 76.3 | 5.9 |
| Aldarondo-Torres et al. 2010 | Jobos Bay, PR | Estuary | 0.06 | 29 | nm | nm | nm | 11 | 64 | 2.6 |
| Apeti et al. 2012 | Jobos Bay, PR | Estuary | 0.01 | 34.4 | 18.4 | 11.1 | 510 | 7.3 | 55 | 2.6 |
| Pait et al. 2008 | La Parguera, PR | Nearshore, Marine | 0.1 | 5.21 | 31.2 | 26.6 | 109 | 1.93 | 7.99 | 5.2 |
| Aceve do-Figueroa et al. 2006 | San José Lagoon, PR | Estuary | 1.8 | 105 | nm | nm | nm | 219 | 531 | 3.9 |
| | Joyuda Lagoon, PR | Estuary | 0.1 | 22 | nm | nm | nm | 7.6 | 52 | 4.9 |
| Whitall et al. 2014 | Guanica Bay, PR | Nearshore, Marine | 0.02 | 29.18 | 286.46 | 228.71 | 470 | 6.08 | 46.71 | 2.7 |
| Jaffe et al. 2003 | Montego Bay, Jamaica | Bay | 5.4 | 44.3 | 22.4 | 16.8 | nm | 30.5 | 59.6 | nm |

nm = not measured

* values are represented as a percentage